

Article

ExoPhot: The Photon Absorption Rate as a New Metric for Quantifying the Exoplanetary Photosynthetic Activity Fitness

Pablo Marcos-Arenal ^{1,2,*}, Luis Cerdán ^{3,†}, Mercedes Burillo-Villalobos ⁴, Nuria Fonseca-Bonilla ², Juan García de la Concepción ², María Ángeles López-Cayuela ⁵, Felipe Gómez ² and José A. Caballero ⁶

¹ HE Space for ESA, ESA/ESAC, Villanueva de la Cañada, 28692 Madrid, Spain

² Centro de Astrobiología (CSIC-INTA), Instituto Nacional de Técnica Aeroespacial, Torrejón de Ardoz, 28850 Madrid, Spain

³ Instituto de Ciencia Molecular (ICMoL), Universidad de Valencia, 46071 Valencia, Spain

⁴ Ingeniería de Sistemas para la Defensa de España (ISDEFE), 28040 Madrid, Spain

⁵ Área de Investigación e Instrumentación Atmosférica, Instituto Nacional de Técnica Aeroespacial, Torrejón de Ardoz, 28850 Madrid, Spain

⁶ Centro de Astrobiología (CSIC-INTA), European Space Astronomy Centre, Villanueva de la Cañada, 28691 Madrid, Spain

* Correspondence: pablo.marcosarenal@esa.int

† These authors contributed equally to this work.



Citation: Marcos-Arenal, P.; Cerdán, L.; Burillo-Villalobos, M.; Fonseca-Bonilla, N.; de la Concepción, J.G.; López-Cayuela, M.Á.; Gómez, F.; Caballero, J.A. ExoPhot: The Photon Absorption Rate as a New Metric for Quantifying the Exoplanetary Photosynthetic Activity Fitness. *Universe* **2022**, *8*, 624. <https://doi.org/10.3390/universe8120624>

Academic Editor: Diego Turrini

Received: 27 October 2022

Accepted: 23 November 2022

Published: 26 November 2022

Publisher's Note: MDPI stays neutral with regard to jurisdictional claims in published maps and institutional affiliations.



Copyright: © 2022 by the authors. Licensee MDPI, Basel, Switzerland. This article is an open access article distributed under the terms and conditions of the Creative Commons Attribution (CC BY) license (<https://creativecommons.org/licenses/by/4.0/>).

Abstract: Only a low percentage of the radiation from our Sun is captured by photosynthesis, but this conversion of solar to chemical energy sustains all life on Earth. Photosynthesis could be present in any exoplanetary system fulfilling the main three ingredients for this metabolic route: light, water, and carbon dioxide. To deepen into this idea, the ExoPhot project aims to study the relation between photosynthetic systems and exoplanet conditions around different types of stars by focusing on two aspects: (i) Assessing the photosynthetic fitness of a variety of photopigments (either found on Earth or theoretical) as a function of stellar spectral type, star-exoplanet separation, and planet atmosphere basic parameters, and (ii) delineating a range of stellar, exoplanet, and atmospheric parameters for which photosynthetic activity might be feasible. In order to address these goals, we make use of a new metric, the absorption rate γ , for the evaluation of the exoplanet photosynthetic activity that, based on state-of-the-art planet atmosphere and stellar photosphere spectroscopic models, quantifies the overlap between those models with the absorption spectra of photosynthetic pigments, both terrestrial and theoretical. We provide with a set of results for a combination of photosystems and exoplanetary environments revealing the importance of our metric when compared to previous photosynthesis indicators.

Keywords: astrobiology; exoplanets; planetary systems; atmospheres; terrestrial planets

1. Introduction

Astrobiology is an interdisciplinary scientific field that integrates concepts of astronomy, biology, chemistry, geology, and physics. Although its name was first coined in 1953 [1], astrobiology has grown very fast in the last decades due to space missions to Solar System planets and moons, the studies of extremophiles on our Earth, and, especially, the discovery and characterization of exoplanets, which began with 51 Pegasi b, the first confirmed exoplanet around a Sun-like star [2]. The latest advances in technology and data analysis allow us now to dream of the exoplanet discoveries that the next generation of facilities and astrobiologists will achieve. With the James Webb Space Telescope now in operation, the Extremely Large Telescope and Giant Magellan Telescope under construction, and PLATO (PLANetary Transits and Oscillations of stars), ARIEL (Atmospheric Remote-sensing Infrared Exoplanet Large-survey), and the Nancy Grace Roman Space Telescope to be launched no later than 2030, we are increasingly closer to the discovery

of the first true Earth analogue, a 1 Earth-mass, 1 Earth-radius planet in orbit at 1 au to a G2 V star. The next generation of space telescopes envisioned by the US Decadal Survey on Astronomy and Astrophysics and the European Space Agency Voyage 2050 plan, still to be defined, will play a pivotal role in the detection of incontrovertible biomarkers in the atmospheres of exo-Earths in the habitable zone (HZ) around their host stars [3–7].

As discussed below, particular emphasis has been placed on the search for biomarkers associated with photosynthesis, the physicochemical process by which plants and other organisms obtain nutrients from water and carbon dioxide [8,9], and it is considered one of the first metabolic routes on the planet. Photosynthesis modified the atmosphere of the early Earth by producing oxygen as a byproduct and transformed the metabolic possibilities for the rest of the organisms [10], so it could also happen on other planets. Photosynthesis could be present in any exoplanet that retains an atmosphere [11,12], orbits the adequate stellar host at the right Goldilocks separation (neither too hot nor too cold, as a wee bear’s porridge; [3]), and have access to light, water, and carbon dioxide. Consequently, the development of astronomical facilities capable of detecting biomarkers associated with photosynthesis could provide further clues about exobiology.

Here, we pave the way for the following generation of facilities that will shed light on the biochemistry of exoplanets’ ecosystems. The overarching goal of the “Photosystems in exoplanets” (ExoPhot¹) project is to study the photosystems that might generate biomarkers and their detectability conditions by a twofold approach: understanding the evolutionary steps that led to the highly evolved chlorophylls and analogues [13] and assessing the feasibility or likelihood to trigger photosynthetic activity in an exoplanetary system (this paper).

The conversion of light to chemical energy through photosynthesis occurs on Earth following different reactions involving a chain of physical and chemical processes, but they are all ignited by the absorption of solar radiation by the photosynthetic pigments [14,15] (photopigments hereafter) in the antenna complexes in the thylakoids of photosynthetic organisms. Accordingly, a key step in assessing the photosynthetic fitness—or how likely it is that a certain “system” (composed of an exoplanet, its atmosphere, its host star, and a determined photopigment) can withstand photosynthetic activity—is to check whether the photopigment would absorb enough light from the host star to trigger the chain reaction. Based on an evolutionary Darwinian hypothesis and assuming long-term, stable, and suitable for life conditions, those photosystems whose light absorption best match the spectral energy distribution of the star at the planet’s surface would be more prone to thriving [6,16]. Thus, the higher this photosynthetic fitness is, the larger the chances are that the photosystem has evolved and, therefore, we can make use of those quantitative parameters to infer how likely is for the exoplanet to host evolved photosynthetic organisms.

Earlier studies have tackled this matter by following different strategies to relate the spectral type of the host star, the composition and properties of the atmosphere of the planet, and the different varieties of photopigments that they might host [10,16–25]. Most of these studies considered the stellar flux density at the surface of Earth-like exoplanets around F-, G-, K-, and, overall, M-type stars (assuming Earth-like or anoxic atmospheres) and compared the flux values with those on Earth. While promising, the scope of these works was still limited, as some of them did not include the effects of the atmosphere, others did not take into consideration the photopigments absorbance, and others were limited to Earth-like exoplanets. Therefore, many questions remain unanswered.

The main aim of the ExoPhot project is to study the relation between photosynthetic systems and exoplanets around different types of stars from an astrobiological and multidisciplinary point of view. In this work, we report a new metric that provides a quantitative value of the photosynthetic fitness of any photopigment in an exoplanet that takes into account the emission spectrum of the host star, the filtering effect of the atmosphere, and the absorptive properties of the photopigment. This metric is applied to the assessment of the photosynthetic fitness of a variety of photopigments (either found on Earth or theo-

retical), as a function of stellar spectral type, exoplanet semi-major axis, and atmospheric composition for which photosynthetic activity might be feasible.

2. Materials and Methods

2.1. Photosynthetic Feasibility Metrics

In order to assess the photosynthetic fitness of a photopigment in a given system, we resorted to metrics that quantify the level of spectral overlap between the photopigment absorption spectrum and the emission spectrum of the host star at the exoplanet surface (i.e., once filtered by its atmosphere). Figure 1 shows an example of the three ingredients required to determine the spectral overlap: the stellar spectral flux density at the top of the exoplanet atmosphere (F_λ), the atmosphere transmittance (\mathcal{T}), and the photopigment absorption cross section (σ_{abs}). The overlap of these three components renders the spectral absorption rate (Γ_λ), which accounts for the number of photons absorbed by a molecule per unit of time and wavelength, and provides quantitative and very insightful information. This parameter is calculated as follows:

$$\Gamma_\lambda(\lambda) = \sigma_{\text{abs}}(\lambda)F_\lambda(\lambda)\mathcal{T}(\lambda)\frac{\lambda}{hc}. \tag{1}$$

The parameter $\sigma_{\text{abs}}(\lambda)$ in Equation (1) is related to the molar extinction coefficient $\epsilon_{\text{abs}}(\lambda)$ through:

$$\sigma_{\text{abs}}(\lambda) = \frac{1000 \log 10}{N_A}\epsilon_{\text{abs}}(\lambda), \tag{2}$$

where N_A is the Avogadro number, and $\sigma_{\text{abs}}(\lambda)$ and $\epsilon_{\text{abs}}(\lambda)$ are given in units of cm^2 and $\text{M}^{-1} \text{cm}^{-1}$, respectively.

We defined \mathcal{T} as the atmosphere transmittance, but other extinction effects on the incident radiation (clouds, haze, water, ice, scattering, etc.) could be easily incorporated into $\mathcal{T}(\lambda)$. However, these possible effects will be the subject of forthcoming publication. Furthermore, photopigment absorption σ_{abs} as used in Equation (1) could implicitly contain the environmental effects and interactions undergone in antenna complexes, such as those with protein fragments, aminoacids, or secondary pigments (carotene, etc.), which can significantly modify their spectroscopic signatures [26]. For demonstration purposes, and for the time being, we will restrict ourselves to photopigments in simple solution or vacuum.

A useful single-valued variable that summarizes the information contained in Γ_λ is the total absorption rate, γ_t (in units of s^{-1}), which is obtained by integrating Equation (1) over all wavelengths. In practice, though, it is integrated only over the wavelength range in which the photopigment absorbs. Furthermore, this range is in general not coincidental with the conventional photosynthetic active radiation (PAR) span (4000–7000 Å) [27]. More importantly, this allows accommodating any spectral range covered by non-Earthly photopigments, increasing the generality and applicability of our approach. This is one of the main differences between the absorption rate γ_t and alternative metrics that rely on the previous bandwidth (see below).

When dealing with hundreds or thousands of trios of star-atmosphere-pigment, the analysis of Γ_λ combinations on a one-by-one basis becomes impractical, whereas the use of γ_t might entail the loss of important information in some cases. Besides this, the absorption spectra of photopigments show bands that are usually clustered around two different spectral regions (Figures 1 and A1). The B band (or Soret band) covers the absorption at the high energy range, while the Q band does the corresponding at the low energy range. Accordingly, for those cases, the total absorption rate (γ_t) can be split into contributions of the B and Q bands (γ_B and γ_Q) as:

$$\gamma_t = \gamma_B + \gamma_Q = \int_0^{\lambda_c} \Gamma_\lambda(\lambda)d\lambda + \int_{\lambda_c}^\infty \Gamma_\lambda(\lambda)d\lambda, \tag{3}$$

where λ_c is the cut-off wavelength separating both bands. This separation allows to recover important information on the absorption bands that would be lost otherwise. In this work, we chose $\lambda_c = 5000 \text{ \AA}$, being a reasonable separator between the higher and lower absorption regions for the five pigments in our sample as illustrated by Figure A1. The absorption rate γ_t (Equations (1) and (3)) bears a resemblance to the photolysis rate J used in atmospheric chemistry [28].

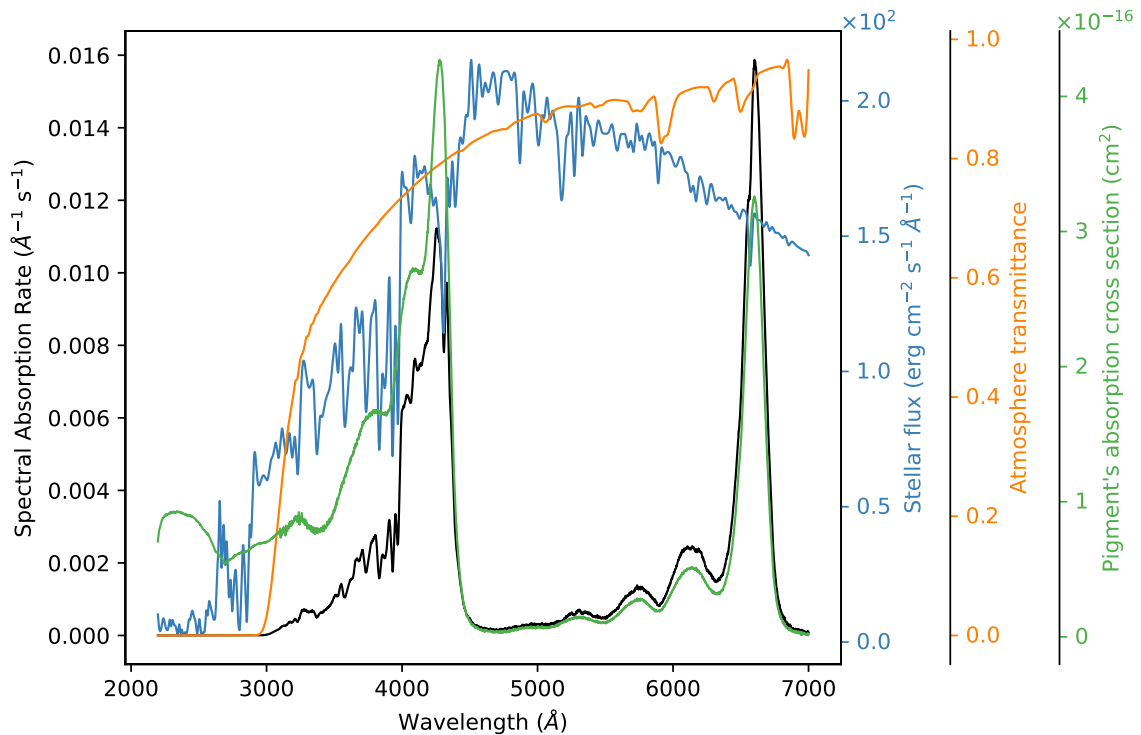


Figure 1. Example of spectral absorption rate calculation: Stellar flux F_λ from a Sun-like star (G2 V) at the top of the planet atmosphere (blue), transmittance (\mathcal{T}) of an Earth-like atmosphere (orange), absorption cross section σ_{abs} of chlorophyll a (green), and spectral absorption rate Γ_λ from the combination of the three previous elements (black).

There are other related metrics that are widely extended, such as the total stellar irradiance (S , in W m^{-2}) at the top of the planet atmosphere, which provides information on the stellar bolometric flux received by a planet at the top of its atmosphere:

$$S = \frac{L_\star}{4\pi a^2} \tag{4}$$

where L_\star is the star luminosity (in W) and a is the exoplanet orbital semi-major axis (in m). As a result, S depends on the stellar spectral type and the star-planet separation, and is independent of the Bond albedo.

Moreover, the photosynthetic photon flux density ($ppfd$) is a standard metric to assess the PAR that quantifies the amount of radiation available for photosynthesis in the range between 4000 and 7000 \AA [27,29,30], expressed in units of $\mu\text{mol photon m}^{-2} \text{s}^{-1}$ and computed as:

$$ppfd = \frac{1}{N_A} \int_{4000}^{7000} F_\lambda(\lambda) \mathcal{T}(\lambda) \frac{\lambda}{hc} d\lambda. \tag{5}$$

2.2. Stellar Spectral Types

We selected a sample of stars that covered all spectral types whose planets could host photosynthetic systems in their atmospheres. In this work, the sample only covers a solar type (G2 V, $T_{\text{eff}} = 5750 \text{ K}$) and two extreme cases at the hot (A5 V, $T_{\text{eff}} = 8250 \text{ K}$) and cool

ends (M8 V, $T_{\text{eff}} = 2500$ K) of the main sequence, while for future development the sample will cover a denser mesh.

The sample does not include stars with spectral types O, B, and early A spectral types (i.e., warmer than $T_{\text{eff}} \approx 8250$ K) because their soft X-ray emission and far ultraviolet radiation eliminate the possibility of complex organic molecule formation in their vicinity. Moreover, these stars reside in the main sequence for only a few tens of millions of years before becoming giant stars and, after a cataclysmic event incompatible with life, concluding as white dwarfs, neutron stars, or even black holes.

On the other hand, we did not include either stars and brown dwarfs with late L, T, and Y spectral types (i.e., cooler than $T_{\text{eff}} \approx 2200$ K) because they are so faint that their HZ lie very close to their Roche radius and, therefore, do not have temperate planets where photosystems can exist [23,31,32]. Exoplanets in the HZ around late-M- and early-L-type dwarfs have very short orbital periods [33–35] and are, thus, tidally locked to their stars, although this fact does not apply to their moons, if retained [36]. Early- and mid-M dwarfs have, in general, a high frequency of flares, which can be intense enough to erode the atmospheres of their planets [37]. However, since there are hints for M-dwarf exoplanet atmospheres even inside the HZ [38], we did consider them in the analysis.

We used the ATLAS9 parameters and models of Castelli and Kurucz [39] to obtain the fluxes of A5 V and G2 V stars, and the BTSettl-CIFIST models of Baraffe et al. [40] with the parameters of Cifuentes et al. [41] for the M8 V star, both with solar metallicities (i.e., $[\text{Fe}/\text{H}] = 0$). We obtained the spectral energy distributions (SEDs) through the Virtual Observatory² SED Analyser (VOSA, [42]). The flux for G2 V is presented in Figure 1, and those for A5 V and M8 V are displayed in Figure A2.

2.3. Modelling of Exoplanets Atmospheres

In order to tackle the wide variety of possible exoplanetary atmospheres, we considered four different scenarios: Earth-like (78% N₂, 21% O₂), highly oxidizing (90% CO₂, 10% N₂), weakly oxidizing (>99% N₂), and reducing (90% H₂, 10% N₂). We took the last three scenarios from Hu et al. [11], while the Earth-like atmosphere was taken from the Planetary Spectrum Generator³ (PSG, [43]). The highly oxidizing atmosphere scenario may correspond, as well, to an early Earth-like exoplanet [44]. This sample was intended to cover a very wide range of possible atmospheres suitable for life, with particular emphasis on the Earth conditions. In all cases, we considered planet scenarios with $1 M_{\oplus}$ and $1 R_{\oplus}$. Again, the study of the variation of the photosynthetic system upon the size of the planet and different atmospheric heights is deferred to forthcoming works.

We placed these scenarios into three different positions on the habitability zone: inner, middle, and outer (HZi, HZm, and HZo), characterized by their equilibrium temperature, T_{eq} (300 K, 255 K, and 240 K, respectively). These temperatures were derived, after setting the Bond albedo (A_{Bond}) at 0.30, from surface temperatures of 333 K (60 °C), 288 K (15 °C), and 273 K (0 °C) after subtraction of a fixed greenhouse effect of 33 K, identical to the currently found on Earth. Although they cover the range between the thermophile limit (60 °C,) and water in a liquid state (0 °C). This thermophile limit approximately coincides with the atmosphere temperature at which an Earth-like planet suffers a runaway greenhouse [3,45].

The exoplanet orbital semi-major axis a at the different HZs corresponding to each spectral type was derived from the radiative equilibrium formula, which relates a with the stellar luminosity L_{\star} , A_{Bond} , and T_{eq} as:

$$a = \sqrt{\frac{L_{\star}(1 - A_{\text{Bond}})}{16\pi\sigma T_{\text{eq}}^4}} \quad (6)$$

where σ is the Stefan-Boltzmann constant. The luminosity is a function of the stellar radius, R_{\star} , and effective temperature, T_{eff} , which depends on the spectral type, through $L_{\star} = 4\pi\sigma R_{\star}^2 T_{\text{eff}}^4$. These values served as input to the atmosphere transmittance calculation.

We used the PSG to synthesize and retrieve the planetary atmospheric transmittances for each of the oxidizing states mentioned above. For each host star, we set its T_{eff} , R_{\star} , and mass (which is an input for the planet surface gravity and, therefore, the atmosphere length scale) according to the parameters determined for its corresponding SED model. The star-planet separation was set as determined for each of the HZs. The resulting transmittance spectra for all possible combinations can be found in Figure A3. For a given atmosphere scenario, there is almost no difference in the atmospheric transmittance between spectral types and ranges of HZs because there are few variations in the exoplanet's parameters in the narrow band of its own HZ.

2.4. Calculation of Absorption Cross-Section of Pigments

We applied Equation (2) to calculate the absorption cross-section of five different photopigments: the existing natural pigments chlorophyll *a* (Chl *a*), chlorophyll *b* (Chl *b*), bacteriochlorophyll *a* (BChl *a*), and bacteriochlorophyll *b* (BChl *b*), and a new theoretical photopigment, namely, Phot0 [13]. The molar extinction coefficient, $\epsilon_{\text{abs}}(\lambda)$, of the natural pigments in diethyl ether was retrieved from the database accompanying the article by Taniguchi and Lindsey [46].

Phot0 is a plausible primeval molecule that shares the spectroscopic characteristics and structural rigidity of common photopigments such as chlorophylls and bacteriochlorophylls, but is much simpler, as it contains only the central macrocycle that surrounds the metallic center [13]. Considering the proposed geochemical conditions (the plume of volcanic eruptions) and raw materials (acetylene and hydrogen cyanide) yielding Phot0, it could be abundant in rocky exoplanets. For the calculation of the ultraviolet and visible (UV/Vis) spectrum of the theoretical pigment Phot0, we followed the same methodology used previously for the calculation of the absorption spectrum of Chl *a* [47]. In short, the vertical excitation energies were computed within the time-dependent formalism with the double hybrid B2PLYP functional on optimized CAM-B3LYP geometries. A total of ten roots were computed, and the transition line widths were set to 0.1 eV. For more details, see García de la Concepción et al. [13]. The resulting absorption cross-section spectra for the five photopigments are displayed in Figure A1.

2.5. Code and Data Availability

We developed Jupyter notebooks describing and implementing all these calculations, together with the Python code required to execute them. Our code takes separated input files for each component (ϵ_{abs} , F_{λ} , \mathcal{T}) as column-separated wavelength value arrays and performs a data preprocessing before computing Equations (1), (3) and (5). The preprocessing step consists of a unit conversion of wavelengths and fluxes, the calculation of σ_{abs} (Equation (2)), a search for the maximum wavelength span for which there are data available for σ_{abs} , F_{λ} , and \mathcal{T} , and a final cubic spline interpolation so that all variables share the same wavelength values. The integration is performed using the standard trapezoidal rule. The original datasets, processing methods and algorithms required to reproduce the figures, tables, and results presented in this work are publicly available on the ExoPhot Github website.⁴

3. Results and Discussion

Table 1 summarizes the resulting values of γ_t , γ_Q , and γ_B obtained for an exoplanet in HZm around a G2 V star. The *ppfd* is provided for comparison purposes. The stellar irradiance is also provided in the caption for completeness. Figure 1 shows an example of Γ_{λ} resulting from the spectral overlap between three components: the stellar flux of a Sun-like star (G2 V) reaching the top of an Earth-like exoplanet, the transmittance of an Earth-like atmosphere, and the absorption cross-section of Chl *a*. Integration over wavelength of the curve Γ_{λ} provides the number of photons per second that Chl *a* absorbs under Earth conditions, resulting in $\gamma_t = 9.20, \text{ s}^{-1}$ (third row of Table 1). In other words, since energy transfer is the dominant de-excitation process of Chl *a* within the antenna

complex [48], this value of γ_t allows inferring that each Chl *a* molecule could contribute up to 9.20 photons per second to the photosynthetic reaction, in agreement with experimental evidence [48].

In addition, as illustrated by Figure 1, the Γ_λ value at the peak of the Q band ($\sim 6600 \text{ \AA}$) is higher than that at the B band ($\sim 4000 \text{ \AA}$), even when its absorbance is weaker. However, in spite of this difference, both bands contribute with a similar number of electrons or absorbed photons ($\gamma_Q = 4.55 \text{ s}^{-1}$ vs. $\gamma_B = 4.65 \text{ s}^{-1}$). Upon absorption of a photon, irrespective of the electronic state involved (e.g., Q, or B band), the excited molecule will undergo a series of ultrafast non-radiative transitions towards the lowest lying electronic excited state, from where the energy transfer takes place. From this perspective, $\gamma_Q \sim \gamma_B$ could be understood as both bands contributing similarly to the overall photosynthetic process. These results highlight the relevance of our metric to explore the photosynthetic fitness, at least from a photophysical point of view.

Table 1. Photosynthetic fitness metrics for Earth-like exoplanets with different atmospheres in the middle of the HZ around a G2 V star ^a.

Exopl. Atmos.	<i>ppfd</i> [$\mu\text{mol photon m}^{-2} \text{ s}^{-1}$]	Pigment	γ_t [s^{-1}]	γ_B [s^{-1}]	γ_Q [s^{-1}]
Earth-like	2115.69	BChl <i>a</i>	11.51	2.47	9.04
		BChl <i>b</i>	14.07	4.54	9.52
		Chl <i>a</i>	9.20	4.65	4.55
		Chl <i>b</i>	11.14	7.51	3.63
		Phot0	6.72	1.33	5.39
Highly oxidizing	1950.40	BChl <i>a</i>	13.35	3.32	10.02
		BChl <i>b</i>	16.30	5.77	10.53
		Chl <i>a</i>	10.82	5.92	4.90
		Chl <i>b</i>	12.90	8.95	3.95
		Phot0	8.00	2.01	5.99
Weakly oxidizing	2168.68	BChl <i>a</i>	12.23	2.46	9.77
		BChl <i>b</i>	14.79	4.50	10.28
		Chl <i>a</i>	9.37	4.65	4.72
		Chl <i>b</i>	11.26	7.48	3.78
		Phot0	7.15	1.32	5.84
Reducing	2338.10	BChl <i>a</i>	11.03	1.64	9.39
		BChl <i>b</i>	13.13	3.21	9.92
		Chl <i>a</i>	7.82	3.36	4.46
		Chl <i>b</i>	9.39	5.84	3.54
		Phot0	6.34	0.73	5.61

^a In all exoplanet atmosphere types, the stellar irradiance (*S*) at the atmosphere top of an exoplanet in HZm around a G2 V star is $1370.042 \text{ W m}^{-2}$.

The application of *ppfd* to assess photosynthetic feasibility in exoplanets is widely extended [20,22,23]. This parameter measures the amount of light that reaches the photosynthetic organism but, as mentioned before, is usually limited to the range between 4000 and 7000 (Equation (5)). However, in view of recent experimental evidence suggesting the feasibility of photosynthetic activity under exclusive far-red radiation [49,50], wider range versions of the *ppfd* are being used [18,24]. Nevertheless, none of them considers pigment absorption, as shown in Table 1. Alternative metrics that explicitly include the absorption properties of the photosynthetic pigment or organism have also been proposed, but do not provide absolute quantitative results [17,19]. Therefore, existing metrics, although aimed in the direction of photosynthetic viability assessment, cannot complete the picture of the whole system as our proposed photosynthetic fitness parameter does. In this sense, the absorption rate, either spectrally resolved (Γ_λ , Equation (1)) or integrated (γ_t , γ_B , and γ_Q , Equation (3)), allows great flexibility to assess the photosynthetic fitness of a given pigment in a star–exoplanet–atmosphere system, and could also serve as an assessment metric for photosynthetic biomarkers.

Besides the absorption rate properties of our simulated modern Earth conditions (G2 V spectral type, HZm, and Earth-like atmosphere), the inner and outer boundaries of the habitable zone (HZi and HZo, respectively, [51]) for the G2 V star are presented in Table A3 as an extended version of Table 1. The results for exoplanets (only in their HZm) around A5 V and M8 V stars are also presented in Tables A2 and A4, respectively. Figure 2 illustrates the photopigments spectral absorption rate, Γ_λ for the 60 combinations of exoplanets in the HZm for A5 V, G2 V, and M8 V stars. This plot (and Tables A2–A4) indicates that, whereas the composition of the atmosphere would have an impact on the photosynthesis chemistry and organisms survival likelihood, it does not have a major influence on the absorption of photons by any pigment or spectral type of star.

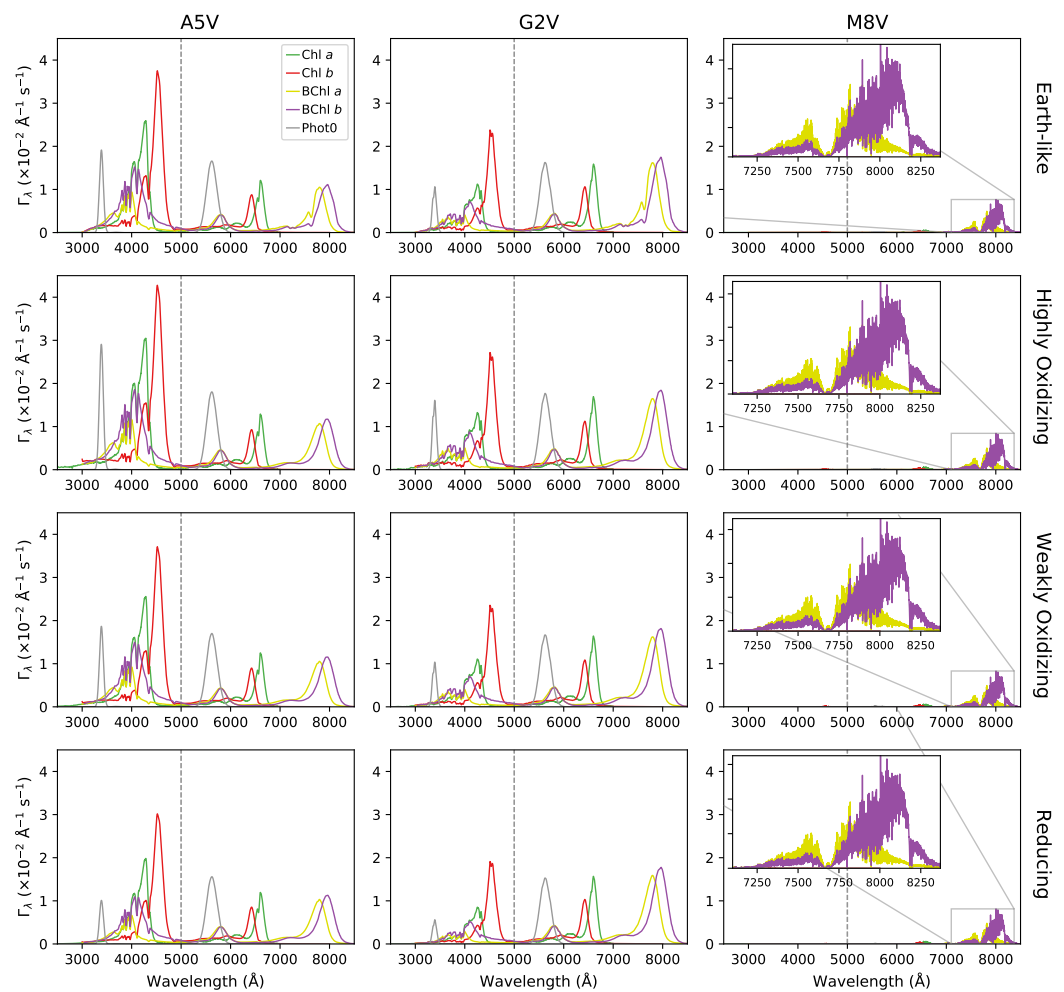


Figure 2. Spectral absorption rates for five photopigments (Chl *a*, Chl *b*, BChl *a*, BChl *b*, and Phot0) on Earth-like exoplanets with four different atmospheres (Earth-like, highly oxidizing, weakly oxidizing, and reducing, in their respective rows) in the HZm around stars of three different spectral types (A5 V, G2 V, and M8 V, in columns). The vertical dashed lines mark the cut-off wavelength separating the Q and B bands at 5000 Å. All panels follow the same color code (cf. upper left panel legend). For the sake of visualization, we smoothed the M8 V star spectra with a 25-point running average and displayed zoom-ins of the region of interest.

Regarding the exoplanet atmosphere composition, variations of around 20% in γ_t are observed regardless of the photopigments, more noticeably in the highest energy band (γ_B). These variations are mainly due to the atmosphere transmittance drop in the B band (see Figure A3), which depends on the composition of the atmosphere. Furthermore, the reducing atmosphere systematically shows the largest values of γ_t , γ_B , and γ_Q (Table 1). Under these conditions, our theoretically proposed photosynthetic primordial pigment,

Phot0, presents absorption rates that are smaller than those observed for more complex photopigments (Table 1), but still sufficiently high to sustain photosynthetic activity [52]. Remarkably, while Phot0 γ_Q values barely change with the atmosphere oxidizing state, its γ_B values vary significantly, being maximized in the reducing atmosphere type (Figure 2). This result suggests that Phot0 could particularly thrive as a photosynthetic pigment in highly oxidizing atmospheres that, incidentally, could serve as an approximate analogue for a primeval Earth [53]. Therefore, these results back up the hypothesis that Phot0 could be a primeval pigment preceding the highly evolved chlorophylls in the early Earth or even young, habitable rocky exoplanets [13], and highlight the relevance and usefulness of the absorption rates to assess the photosynthetic fitness in an exoplanetary context. Analogous results and trends are observed for exoplanets in the HZo and HZi of G2 V stars, as well as those orbiting A5 V and M8 V stars in HZm (Tables A2–A4).

In relation to the location of the exoplanet within the HZ, moving away from the star diminishes the amount of light available for photosynthesis. This is noticeable by comparing both γ_t and *ppfd* for different atmosphere types for the inner, middle, and outer HZ of G2 V stars (see Table A3). Nevertheless, the *ppfd* at the outer boundary is enough to perform photosynthesis. In fact, in Earth-based photosynthetic systems, the CO₂ assimilation, which is a manifestation of photosynthesis, starts to saturate around those *ppfd* values, meaning that the amount of light is so high that it puts at risk the survival of the photosystem as a whole. Accordingly, the standard HZ definition based on the existence of liquid water is more stringent than that of the existence of photosynthesis, at least in G-type stars.

M dwarfs are the most common stars in our galaxy [54,55] and thus have received a great deal of attention in the study of exoplanetary photosynthesis [18–20,22]. These studies, mostly based on evaluations of *ppfd*, concluded that, in general, oxygenic photosynthesis could not be successful in mid and late M stars. The *ppfd* for exoplanets orbiting M8 V dwarfs in HZm is below 20 $\mu\text{mol photon m}^{-2} \text{s}^{-1}$ (Table A4), an amount considered insufficient for higher plants based on the common Earth (they would be in the dark respiration rate region where CO₂ is released [30]). This low *ppfd* would translate into no photosynthesis, at least for higher plants based on chlorophylls, but it could be otherwise for hypothetical bacteriochlorophyll-based plants and/or bacteria. In fact, some organisms have been found sustaining photosynthetic activity at *ppfd* values down to 0.01 $\mu\text{mol photon m}^{-2} \text{s}^{-1}$ [52]). However, our study shows that the sole contribution to the absorption rates in M stars comes from the Q bands (longer wavelengths in Figure 2) as the stellar emission in the B band is negligible. The absorption rate in the Q band ascends to approximately 1 s^{-1} , at least for BChl *a* and *b* (Table 1). This value is on par with the total absorption rate (Q+B bands) that would experience both BChls on Earth under a *ppfd* of approximately 200 $\mu\text{mol photon m}^{-2} \text{s}^{-1}$ (cf. Table 1), which is sufficient to activate photosynthesis [30,52]. Thus, if we followed the advice of the *ppfd*, the hypothesis of the feasibility of the photosynthetic activity on M8 V stars would be rejected, but our metric suggests otherwise. The relevance of our proposed metric is again highlighted to account for new factors and to draw meaningful conclusions that, in this particular case, are in line with recent laboratory results proving that the growth and photosynthetic activity of cyanobacteria under simulated M7 V-type stars irradiation is possible [50]. The situation would be more favorable if the exoplanet did orbit closer to the star, where the radiation is stronger. Furthermore, it has been suggested that the radiation resulting from flares in M dwarfs could even help sustain photosynthetic activity [19]. Finally, the evolutionary pressure exerted by the dim illumination conditions might lead to the survival of photosynthetic antennae with a larger number of chromophoric units per complex, and/or a larger number of antenna complexes per reaction center, as compared with Earth-based systems. Accordingly, the existence of photosynthetic activity in exoplanets orbiting M dwarfs cannot simply be ruled out by inspecting the *ppfd*.

The total absorption rates (γ_t) in exoplanets orbiting the HZm of A5 V and G2 V stars are very similar irrespective of the type of atmosphere and pigment (Table A3), even when the former stars intrinsically emit more photons than the latter ones. Two facts contribute

to this similarity: the star-planet separation at HZm is shorter in G2 V stars, and their atmospheres absorb most of the UV radiation, where the difference in flux between A5 V and G2 V stars is the highest (see Figure A2). The combination of these two facts results in a drastic decrease in the number of photons arriving at the exoplanet surface. In any case, in A5 V stars, the maximum contribution to the spectral absorption rate Γ_λ comes from the energetic B band (Figure 2), but it does not necessarily translate into $\gamma_B > \gamma_Q$ in general (Table A3); there are atmospheres and pigments combinations where actually the opposite is true. The fact that the main contribution to photosynthesis comes from the Q band [29] could mean that, even when there is more radiation in A-type stars, there could be less photosynthetic activity. This is another case where our γ metric becomes useful.

4. Conclusions

A new metric for assessing the feasibility or likelihood to identify photosynthetic activity in an exoplanetary system has been presented as a cornerstone of the ExoPhot project. This metric, the total absorption rate, γ_t , quantifies the level of spectral overlap between the absorption spectrum of a photosynthetic pigment, the transmittance spectra of an exoplanet atmosphere, and the emission spectrum of its host star. Therefore, it can shed light on the potential biochemistry of exoplanet ecosystems, the biomarkers that might generate, and their detectability conditions. It can also be considered an indicator of the evolutionary path of primeval pigments and can help us understand the steps that led to highly evolved chlorophylls and analogues [13], being this research line the twofold aim of the ExoPhot project.

Compared to other widely extended related metrics such as S and $ppfd$, γ_t (and γ_B and γ_Q) provides more meaningful information in terms of photosynthetic activity. The former metrics solely rely on the net radiation received by an exoplanet—at its top atmosphere (S) or surface ($ppfd$)—for comparing the photosynthetic viability as a function of the separation between star and exoplanet, stellar type, and planet atmosphere. The γ_t allows these comparisons but, on top of that, can discriminate which pigment is more suitable for each case. In this work, we demonstrate that an A5 V star is not necessarily more prone to photosynthesis than a G2 V in spite of emitting more flux, since it depends on the pigment. The same conclusion stands for different exoplanet atmospheres with respect to the pigments, and the other way around: BChl b is the most favorable pigment for an exoplanet around a G2 V star, irrespective of the exoplanet atmosphere. But that is not the case for an A5 V star, where Chl b presents a higher γ_t value.

The ExoPhot project will be extending the number of photosynthetic pigments, stellar spectral types, exoplanets separations and atmospheres in which to evaluate the photosynthetic fitness parameters. More precisely, we intend to cover all known chlorophyll analogues on Earth [46] plus some other theoretical pigments precursors of them [13]. This project will continue extending the range of parameters to be considered in order to refine the most likely family of pigments to exist in a concrete system. It might, therefore, give hints to the spectral features in exoplanets that we must search for when the facilities for discerning them are available. Before that, however, there are many other questions to be tackled, such as if BChl b , present in purple bacteria, would be the “fittest” pigment for temperate rocky exoplanets around M dwarfs, the most abundant stars in our Galaxy; if the metallicity of the host star could affect the planet’s biochemistry and its atmosphere composition; if pigments could have zinc instead of magnesium in the center of their cyclic tetrapyrrole rings; or what the best wavelength range for observing the corresponding absorption features would be.

Author Contributions: F.G. and J.A.C. designed the research; P.M.-A., L.C., M.B.-V., N.F.-B., J.G.d.l.C. and M.Á.L.-C. performed the research and analyzed data; P.M.-A. and L.C. wrote the paper. All authors have read and agreed to the published version of the manuscript.

Funding: We acknowledge financial support from the Agencia Estatal de Investigación of the Ministerio de Ciencia e Innovación and the European Regional Development Fund “A way of making Europe” through projects PID2019-105552RB-C41, PID2019-109522GB-C51, and the Centre of Excellence “María de Maeztu” award to the Centro de Astrobiología (MDM-2017-0737), and from the Instituto Nacional de Técnica Aeroespacial through project S.IGS22001 and a predoctoral contract.

Data Availability Statement: Publicly available datasets were analyzed in this study. These data can be found here: <http://github.com/ExoPhotProject> (accessed on 22 November 2022).

Acknowledgments: We gratefully thank the Research & Technological Innovation and Supercomputing Center of Extremadura (CénitS) for allowing us the use of LUSITANIA computer resources.

Conflicts of Interest: The authors declare no conflict of interest.

Abbreviations

The following abbreviations are used in this manuscript:

Chl <i>a</i>	chlorophyll a
Chl <i>b</i>	chlorophyll b
BChl <i>a</i>	bacteriochlorophyll a
BChl <i>b</i>	bacteriochlorophyll b
Phot0	synthetic photosystem 0
<i>ppfd</i>	photosynthetic photon flux density
HZ	habitability zone
HZi	inner part of the HZ
HZm	middle part of the HZ
HZo	outer part of the HZ
PAR	photosynthetic active radiation
<i>S</i>	stellar irradiance
au	astronomical unit

Appendix A. Figures and Tables

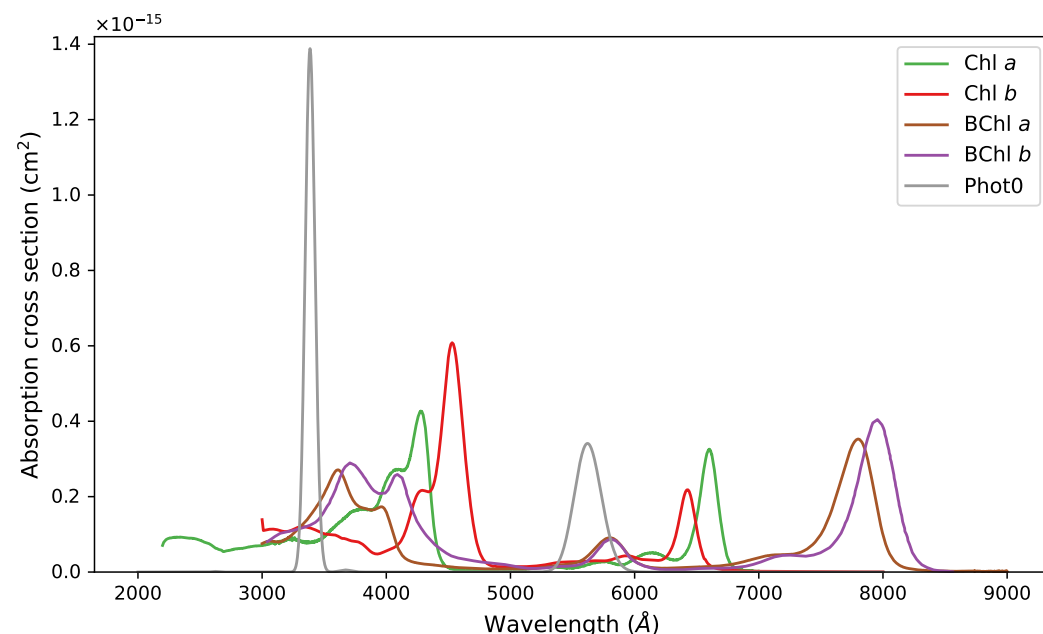


Figure A1. Spectra of the calculated absorption cross sections of the photopigments used in the overlap: Chl *a* (green), Chl *b* (red), BChl *a* (brown), BChl *b* (magenta), and Phot0 (gray).

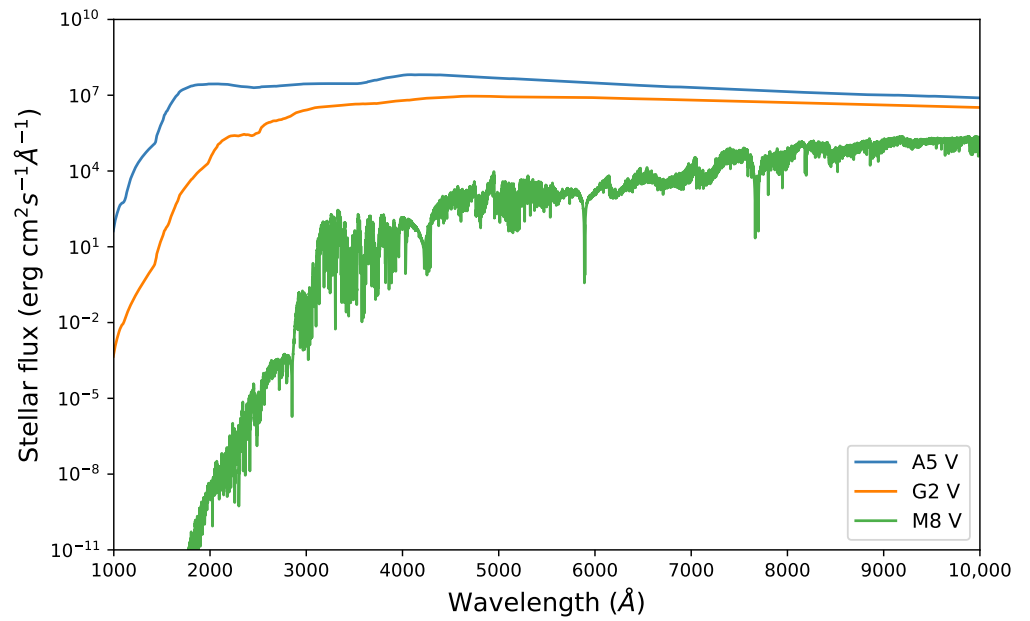


Figure A2. Spectral energy distribution from the far ultraviolet to the near infrared of the A5 V-, G2 V-, and M8 V-type stars used in the overlap.

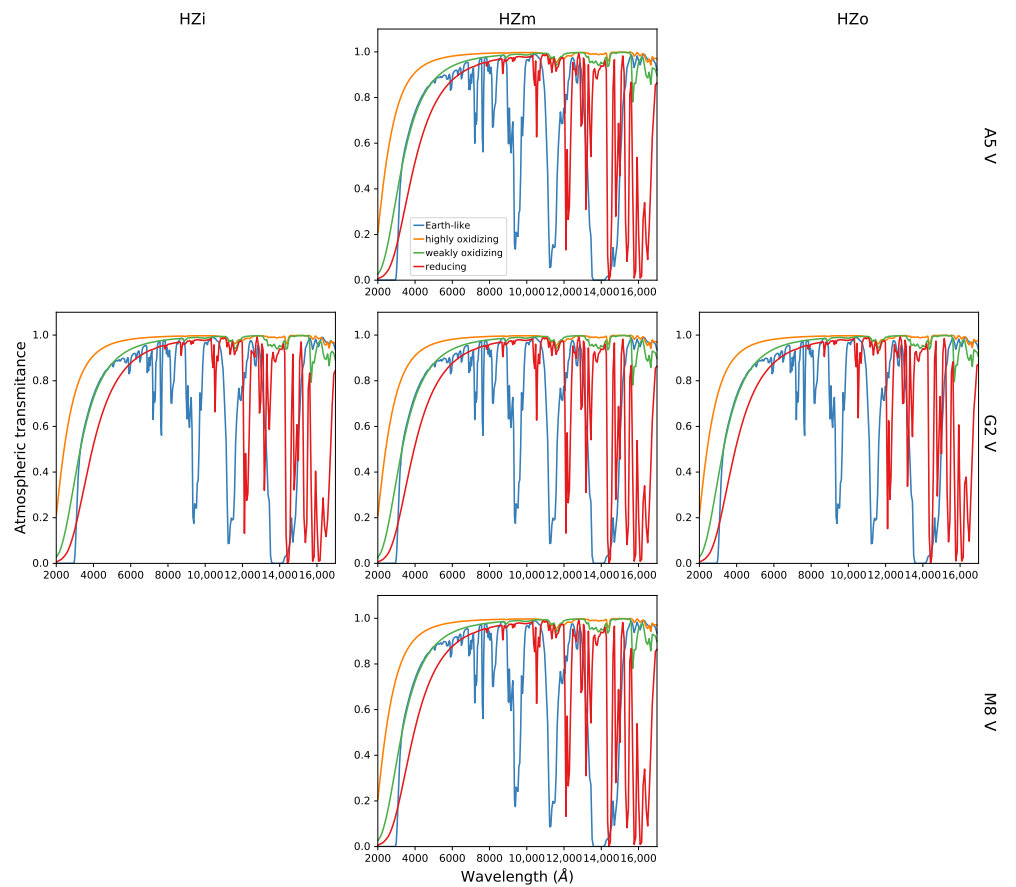


Figure A3. Atmospheric transmittance of exoplanets for different stellar spectral types and planet separations. *Middle column:* Transmittance in the middle of the exoplanet habitable zone (HZm) for A5 V, G2 V, and M8 V stars. *Left and right columns:* Inner and outer habitable zones (HZi and HZo, respectively) for a G2 V star.

Table A1. Stellar parameters, exoplanet separations at inner, medium, and outer HZs, and corresponding irradiances.

Spectral Type	T_{eff} [K]	R [R_{\odot}]	L [L_{\odot}]	HZi [au]	HZm [au]	HZo [au]	S_{HZi} [W m^{-2}]	S_{HZm} [W m^{-2}]	S_{HZo} [W m^{-2}]
A5 V	8250	1.70	12.08	2.50	3.46	3.91	2624.57	1370.04	1075.02
G2 V	5750	1.00	0.99	0.71	0.99 ^a	1.12	2624.57	1370.04	1075.02
M8 V	2500	0.12	5.2×10^{-4}	0.02	0.02	0.02	2624.57	1370.04	1075.02

^a The separation at the middle of the habitable zone, HZm, is different from unity due the use of a standard G2 V model instead of an Earth model.

Table A2. Photosynthetic fitness metrics for Earth-like exoplanets with different atmospheres at the middle of the habitable zone (HZm) around an A5 V star.

Exoplanet Atmosphere	Pigment	γ_t [s^{-1}]	γ_B [s^{-1}]	γ_Q [s^{-1}]	$ppfd$ [$\mu\text{mol photon m}^{-2} \text{s}^{-1}$]	S [W m^{-2}]
Earth-like	BChlA	11.42	4.78	6.65	2400.48	1370.04
	BChlB	15.68	8.92	6.77	2400.48	1370.04
	ChlA	13.54	9.79	3.75	2400.48	1370.04
	ChlB	16.24	12.96	3.27	2400.48	1370.04
	Phot0	6.37	1.91	4.46	2400.48	1370.04
Highly oxidizing	BChlA	10.06	3.20	6.87	2146.82	1370.04
	BChlB	13.31	6.29	7.02	2146.82	1370.04
	ChlA	10.78	7.12	3.66	2146.82	1370.04
	ChlB	13.21	10.03	3.18	2146.82	1370.04
	Phot0	5.23	1.01	4.22	2146.82	1370.04
Weakly oxidizing	BChlA	11.93	4.76	7.17	2442.12	1370.04
	BChlB	16.14	8.83	7.31	2442.12	1370.04
	ChlA	13.76	9.88	3.88	2442.12	1370.04
	ChlB	16.32	12.92	3.40	2442.12	1370.04
	Phot0	6.47	1.87	4.60	2442.12	1370.04
Reducing	BChlA	13.77	6.39	7.38	2676.98	1370.04
	BChlB	18.80	11.30	7.51	2676.98	1370.04
	ChlA	16.77	12.73	4.04	2676.98	1370.04
	ChlB	19.10	15.54	3.56	2676.98	1370.04
	Phot0	7.78	2.90	4.88	2676.98	1370.04

Table A3. Photosynthetic fitness metrics for Earth-like exoplanets with different atmospheres at different separations (HZi, HZm, HZo) around a G2 V star.

HZ	Exoplanet Atmosphere	Pigment	γ_t [s^{-1}]	γ_B [s^{-1}]	γ_Q [s^{-1}]	$ppfd$ [$\mu\text{mol photon m}^{-2} \text{s}^{-1}$]	S [W m^{-2}]
HZi	Earth-like	BChlA	22.05	4.73	17.32	4052.63	2624.57
HZi		BChlB	26.94	8.71	18.24	4052.63	2624.57
HZi		ChlA	17.63	8.91	8.72	4052.63	2624.57
HZi		ChlB	21.35	14.39	6.96	4052.63	2624.57
HZi		Phot0	10.42	2.07	8.35	4052.63	2624.57
HZi	Highly oxidizing	BChlA	21.16	3.15	18.00	3741.48	2624.57
HZi		BChlB	25.19	6.17	19.02	3741.48	2624.57
HZi		ChlA	15.02	6.47	8.56	3741.48	2624.57
HZi		ChlB	18.02	11.23	6.79	3741.48	2624.57
HZi		Phot0	9.01	1.11	7.90	3741.48	2624.57

Table A3. Cont.

HZ	Exoplanet Atmosphere	Pigment	γ_t [s ⁻¹]	γ_B [s ⁻¹]	γ_Q [s ⁻¹]	<i>ppfd</i> [$\mu\text{mol photon m}^{-2} \text{s}^{-1}$]	S [W m ⁻²]
HZi	Weakly oxidizing	BChlA	23.44	4.73	18.72	4157.44	2624.57
HZi		BChlB	28.35	8.64	19.71	4157.44	2624.57
HZi		ChlA	17.98	8.94	9.04	4157.44	2624.57
HZi		ChlB	21.59	14.35	7.25	4157.44	2624.57
HZi		Phot0	10.65	2.04	8.62	4157.44	2624.57
HZi	Reducing	BChlA	25.57	6.37	19.20	4480.02	2624.57
HZi		BChlB	31.23	11.06	20.17	4480.02	2624.57
HZi		ChlA	20.73	11.34	9.39	4480.02	2624.57
HZi		ChlB	24.73	17.16	7.57	4480.02	2624.57
HZi		Phot0	12.30	3.16	9.14	4480.02	2624.57
HZm	Earth-like	BChlA	11.51	2.47	9.04	2115.69	1370.04
HZm		BChlB	14.07	4.54	9.52	2115.69	1370.04
HZm		ChlA	9.20	4.65	4.55	2115.69	1370.04
HZm		ChlB	11.14	7.51	3.63	2115.69	1370.04
HZm		Phot0	5.44	1.08	4.36	2115.69	1370.04
HZm	Highly oxidizing	BChlA	11.03	1.64	9.39	1950.40	1370.04
HZm		BChlB	13.13	3.21	9.92	1950.40	1370.04
HZm		ChlA	7.82	3.36	4.46	1950.40	1370.04
HZm		ChlB	9.39	5.84	3.54	1950.40	1370.04
HZm		Phot0	4.70	0.57	4.12	1950.40	1370.04
HZm	Weakly oxidizing	BChlA	12.23	2.46	9.77	2168.68	1370.04
HZm		BChlB	14.79	4.50	10.28	2168.68	1370.04
HZm		ChlA	9.37	4.65	4.72	2168.68	1370.04
HZm		ChlB	11.26	7.48	3.78	2168.68	1370.04
HZm		Phot0	5.55	1.06	4.50	2168.68	1370.04
HZm	Reducing	BChlA	13.35	3.32	10.02	2338.10	1370.04
HZm		BChlB	16.30	5.77	10.53	2338.10	1370.04
HZm		ChlA	10.82	5.92	4.90	2338.10	1370.04
HZm		ChlB	12.90	8.95	3.95	2338.10	1370.04
HZm		Phot0	6.42	1.65	4.77	2338.10	1370.04
HZo	Earth-like	BChlA	9.03	1.94	7.10	1660.29	1075.02
HZo		BChlB	11.04	3.57	7.47	1660.29	1075.02
HZo		ChlA	7.22	3.65	3.57	1660.29	1075.02
HZo		ChlB	8.74	5.89	2.85	1660.29	1075.02
HZo		Phot0	4.27	0.85	3.42	1660.29	1075.02
HZo	Highly oxidizing	BChlA	8.68	1.30	7.38	1534.67	1075.02
HZo		BChlB	10.33	2.54	7.79	1534.67	1075.02
HZo		ChlA	6.17	2.66	3.51	1534.67	1075.02
HZo		ChlB	7.40	4.61	2.79	1534.67	1075.02
HZo		Phot0	3.70	0.46	3.24	1534.67	1075.02
HZo	Weakly oxidizing	BChlA	9.61	1.94	7.67	1704.13	1075.02
HZo		BChlB	11.62	3.55	8.07	1704.13	1075.02
HZo		ChlA	7.37	3.67	3.70	1704.13	1075.02
HZo		ChlB	8.86	5.89	2.97	1704.13	1075.02
HZo		Phot0	4.37	0.84	3.53	1704.13	1075.02
HZo	Reducing	BChlA	10.48	2.61	7.87	1835.42	1075.02
HZo		BChlB	12.80	4.53	8.26	1835.42	1075.02
HZo		ChlA	8.49	4.65	3.85	1835.42	1075.02
HZo		ChlB	10.13	7.03	3.10	1835.42	1075.02
HZo		Phot0	5.04	1.30	3.74	1835.42	1075.02

Table A4. Photosynthetic fitness metrics for Earth-like exoplanets with different atmospheres at the middle of the habitable zone (HZm) around a M8 V star.

Exoplanet Atmosphere	Pigment	γ_t [s ⁻¹]	γ_B [s ⁻¹]	γ_Q [s ⁻¹]	<i>ppfd</i> [$\mu\text{mol photon m}^{-2} \text{s}^{-1}$]	<i>S</i> [W m ⁻²]
Earth-like	BChlA	0.95	1.42×10^{-3}	0.94	16.48	1370.04
	BChlB	1.63	3.59×10^{-3}	1.62	16.48	1370.04
	ChlA	0.07	2.20×10^{-3}	0.07	16.48	1370.04
	ChlB	0.06	1.46×10^{-2}	0.05	16.48	1370.04
	Phot0	0.02	2.99×10^{-4}	0.02	16.48	1370.04
Highly oxidizing	BChlA	0.98	1.09×10^{-3}	0.98	16.07	1370.04
	BChlB	1.75	2.84×10^{-3}	1.75	16.07	1370.04
	ChlA	0.07	1.67×10^{-3}	0.07	16.07	1370.04
	ChlB	0.06	1.18×10^{-2}	0.04	16.07	1370.04
	Phot0	0.02	1.56×10^{-4}	0.02	16.07	1370.04
Weakly oxidizing	BChlA	1.01	1.41×10^{-3}	1.01	17.17	1370.04
	BChlB	1.79	3.57×10^{-3}	1.79	17.17	1370.04
	ChlA	0.07	2.17×10^{-3}	0.07	17.17	1370.04
	ChlB	0.06	1.45×10^{-2}	0.05	17.17	1370.04
	Phot0	0.02	2.93×10^{-4}	0.02	17.17	1370.04
Reducing	BChlA	1.03	1.72×10^{-3}	1.03	17.98	1370.04
	BChlB	1.82	4.20×10^{-3}	1.82	17.98	1370.04
	ChlA	0.08	2.62×10^{-3}	0.07	17.98	1370.04
	ChlB	0.07	1.67×10^{-2}	0.05	17.98	1370.04
	Phot0	0.02	4.64×10^{-4}	0.02	17.98	1370.04

Notes

- Further information on the ExoPhot project, data, and processing details can be found at <http://github.com/ExoPhotProject> (accessed on 22 November 2022).
- <http://svo2.cab.inta-csic.es/theory/vosa/> (accessed on 22 November 2022).
- <https://psg.gsfc.nasa.gov/> (accessed on 22 November 2022).
- <http://github.com/ExoPhotProject> (accessed on 22 November 2022).

References

- Cockell, C.S. ‘Astrobiology’ and the ethics of new science. *Interdiscip. Sci. Rev.* **2001**, *26*, 90–96. [[CrossRef](#)]
- Mayor, M.; Queloz, D. A Jupiter-mass companion to a solar-type star. *Nature* **1995**, *378*, 355–359. [[CrossRef](#)]
- Kasting, J.F.; Whitmire, D.P.; Reynolds, R.T. Habitable Zones around Main Sequence Stars. *Icarus* **1993**, *101*, 108–128. [[CrossRef](#)] [[PubMed](#)]
- Sagan, C.; Thompson, W.R.; Carlson, R.; Gurnett, D.; Hord, C. A search for life on Earth from the Galileo spacecraft. *Nature* **1993**, *365*, 715–721. [[CrossRef](#)]
- Des Marais, D.J.; Harwit, M.O.; Jucks, K.W.; Kasting, J.F.; Lin, D.N.C.; Lunine, J.I.; Schneider, J.; Seager, S.; Traub, W.A.; Wolf, N.J. Remote Sensing of Planetary Properties and Biosignatures on Extrasolar Terrestrial Planets. *Astrobiology* **2002**, *2*, 153–181. [[CrossRef](#)]
- Schwieterman, E.W.; Kiang, N.Y.; Parenteau, M.N.; Harman, C.E.; DasSarma, S.; Fisher, T.M.; Arney, G.N.; Hartnett, H.E.; Reinhard, C.T.; Olson, S.L.; et al. Exoplanet Biosignatures: A Review of Remotely Detectable Signs of Life. *Astrobiology* **2018**, *18*, 663–708. [[CrossRef](#)]
- Quanz, S.P.; Ottiger, M.; Fontanet, E.; Kammerer, J.; Menti, F.; Dannert, F.; Gheorghe, A.; Absil, O.; Airapetian, V.S.; Alei, E.; et al. Large Interferometer For Exoplanets (LIFE). *Astron. Astrophys.* **2022**, *664*, A21. [[CrossRef](#)]
- Hall, D.O.; Rao, K. *Photosynthesis*; Cambridge University Press: Cambridge, UK, 1999.
- Blankenship, R.E. *Molecular Mechanisms of Photosynthesis*; John Wiley & Sons: Chichester, UK, 2021.
- Gale, J.; Wandel, A. The potential of planets orbiting red dwarf stars to support oxygenic photosynthesis and complex life. *Int. J. Astrobiol.* **2017**, *16*, 1–9. [[CrossRef](#)]
- Hu, R.; Seager, S.; Bains, W. Photochemistry in Terrestrial Exoplanet Atmospheres. I. Photochemistry Model and Benchmark Cases. *Astrophys. J.* **2012**, *761*, 166. [[CrossRef](#)]
- Trifonov, T.; Caballero, J.; Morales, J.; Seifahrt, A.; Ribas, I.; Reiners, A.; Bean, J.; Luque, R.; Parviainen, H.; Pallé, E.; et al. A nearby transiting rocky exoplanet that is suitable for atmospheric investigation. *Science* **2021**, *371*, 1038–1041. [[CrossRef](#)]

13. García de la Concepción, J.; Cerdán, L.; Marcos-Arenal, P.; Burillo-Villalobos, M.; Fonseca-Bonilla, N.; Lizcano-Vaquero, R.; Ángeles López-Cayuela, M.; Gómez, F.; Caballero, J.A. Phot0, a plausible primeval pigment on Earth and rocky exoplanets. *Phys. Chem. Chem. Phys.* **2022**, *24*, 16979–16987. [[CrossRef](#)] [[PubMed](#)]
14. Berdyugina, S.V.; Kuhn, J.R.; Harrington, D.M.; Šantl Temkiv, T.; Messersmith, E.J. Remote sensing of life: Polarimetric signatures of photosynthetic pigments as sensitive biomarkers. *Int. J. Astrobiol.* **2016**, *15*, 45–56. [[CrossRef](#)]
15. Kolokolova, L.; Hough, J.H.; Levasseur-Regourd, A.C. *Polarimetry of Stars and Planetary Systems*; Cambridge University Press: Cambridge, UK, 2015.
16. Kiang, N.Y.; Segura, A.; Tinetti, G.; Govindjee.; Blankenship, R.E.; Cohen, M.; Siefert, J.; Crisp, D.; Meadows, V.S. Spectral Signatures of Photosynthesis. II. Coevolution with Other Stars And The Atmosphere on Extrasolar Worlds. *Astrobiology* **2007**, *7*, 252–274. [[CrossRef](#)] [[PubMed](#)]
17. Komatsu, Y.; Umemura, M.; Shoji, M.; Kayanuma, M.; Yabana, K.; Shiraishi, K. Light absorption efficiencies of photosynthetic pigments: The dependence on spectral types of central stars. *Int. J. Astrobiol.* **2015**, *14*, 505–510. [[CrossRef](#)]
18. Ritchie, R.J.; Larkum, A.W.; Ribas, I. Could photosynthesis function on Proxima Centauri b? *Int. J. Astrobiol.* **2018**, *17*, 147–176. [[CrossRef](#)]
19. Mullan, D.J.; Bais, H.P. Photosynthesis on a Planet Orbiting an M Dwarf: Enhanced Effectiveness during Flares. *Astrophys. J.* **2018**, *865*, 101. [[CrossRef](#)]
20. Lehmer, O.R.; Catling, D.C.; Parenteau, M.N.; Hoehler, T.M. The Productivity of Oxygenic Photosynthesis around Cool, M Dwarf Stars. *Astrophys. J.* **2018**, *859*, 171. [[CrossRef](#)]
21. Lehmer, O.R.; Catling, D.C.; Parenteau, M.N.; Kiang, N.Y.; Hoehler, T.M. The Peak Absorbance Wavelength of Photosynthetic Pigments Around Other Stars From Spectral Optimization. *Front. Astron. Space Sci.* **2021**, *8*, 689441. [[CrossRef](#)]
22. Lingam, M.; Loeb, A. Photosynthesis on habitable planets around low-mass stars. *Mon. Not. RAS* **2019**, *485*, 5924–5928. Available online: <https://academic.oup.com/mnras/article-pdf/485/4/5924/28271824/stz847.pdf> (accessed on 22 November 2022). [[CrossRef](#)]
23. Lingam, M.; Loeb, A. Constraints on Aquatic Photosynthesis for Terrestrial Planets around Other Stars. *Astrophys. J.* **2020**, *889*, 115. [[CrossRef](#)]
24. Covone, G.; Ienco, R.M.; Cacciapuoti, L.; Inno, L. Efficiency of the oxygenic photosynthesis on Earth-like planets in the habitable zone. *Mon. Not. RAS* **2021**, *505*, 3329–3335. Available online: <https://academic.oup.com/mnras/article-pdf/505/3/3329/38673779/stab1357.pdf> (accessed on 22 November 2022). [[CrossRef](#)]
25. Lingam, M.; Balbi, A.; Mahajan, S.M. Excitation Properties of Photopigments and Their Possible Dependence on the Host Star. *Astrophys. J.* **2021**, *921*, L41. [[CrossRef](#)]
26. Mondragón-Solórzano, G.; Sandoval-Lira, J.; Nochebuena, J.; Cisneros, G.A.; Barroso-Flores, J. Electronic Structure Effects Related to the Origin of the Remarkable Near-Infrared Absorption of *Blastochloris viridis*’ Light Harvesting 1-Reaction Center Complex. *J. Chem. Theory Comput.* **2022**, *18*, 4555–4564. [[CrossRef](#)] [[PubMed](#)]
27. McCree, K. Test of current definitions of photosynthetically active radiation against leaf photosynthesis data. *Agric. Meteorol.* **1972**, *10*, 443–453. [[CrossRef](#)]
28. Madronich, S. Photodissociation in the atmosphere: 1. Actinic flux and the effects of ground reflections and clouds. *J. Geophys. Res. Atmos.* **1987**, *92*, 9740–9752. Available online: <https://agupubs.onlinelibrary.wiley.com/doi/pdf/10.1029/JD092iD08p09740> (accessed on 22 November 2022). [[CrossRef](#)]
29. McCree, K. The action spectrum, absorptance and quantum yield of photosynthesis in crop plants. *Agric. Meteorol.* **1971**, *9*, 191–216. [[CrossRef](#)]
30. Liu, J.; van Iersel, M.W. Photosynthetic Physiology of Blue, Green, and Red Light: Light Intensity Effects and Underlying Mechanisms. *Front. Plant Sci.* **2021**, *12*, 328. [[CrossRef](#)]
31. Desidera, S. Properties of Hypothetical Planetary Systems around the Brown Dwarf Gliese 229B. *Publ. ASP* **1999**, *111*, 1529–1538. [[CrossRef](#)]
32. Caballero, J.A. Formation, Evolution and Multiplicity of Brown Dwarfs and Giant Exoplanets. *Astrophys. Space Sci. Proc.* **2010**, *14*, 79–90. [[CrossRef](#)]
33. Gillon, M.; Jehin, E.; Lederer, S.M.; Delrez, L.; de Wit, J.; Burdanov, A.; Van Grootel, V.; Burgasser, A.J.; Triaud, A.H.M.J.; Opitom, C.; et al. Temperate Earth-sized planets transiting a nearby ultracool dwarf star. *Nature* **2016**, *533*, 221–224. [[CrossRef](#)] [[PubMed](#)]
34. Gillon, M.; Triaud, A.H.M.J.; Demory, B.O.; Jehin, E.; Agol, E.; Deck, K.M.; Lederer, S.M.; de Wit, J.; Burdanov, A.; Ingalls, J.G.; et al. Seven temperate terrestrial planets around the nearby ultracool dwarf star TRAPPIST-1. *Nature* **2017**, *542*, 456–460. [[CrossRef](#)] [[PubMed](#)]
35. Zechmeister, M.; Dreizler, S.; Ribas, I.; Reiners, A.; Caballero, J.A.; Bauer, F.F.; Béjar, V.J.S.; González-Cuesta, L.; Herrero, E.; Lalitha, S.; et al. The CARMENES search for exoplanets around M dwarfs. Two temperate Earth-mass planet candidates around Teegarden’s Star. *Astron. Astrophys.* **2019**, *627*, A49. [[CrossRef](#)]
36. Martínez-Rodríguez, H.; Caballero, J.A.; Cifuentes, C.; Piro, A.L.; Barnes, R. Exomoons in the Habitable Zones of M Dwarfs. *Astrophys. J.* **2019**, *887*, 261. [[CrossRef](#)]
37. Scaló, J.; Kaltenecker, L.; Segura, A.G.; Fridlund, M.; Ribas, I.; Kulikov, Y.N.; Grenfell, J.L.; Rauer, H.; Odert, P.; Leitzinger, M.; et al. M Stars as Targets for Terrestrial Exoplanet Searches And Biosignature Detection. *Astrobiology* **2007**, *7*, 85–166. [[CrossRef](#)] [[PubMed](#)]

38. Caballero, J. A.; González-Álvarez, E.; Brady, M.; Trifonov, T.; Ellis, T. G.; Dorn, C.; Cifuentes, C.; Molaverdikhani, K.; Bean, J. L.; Boyajian, T.; et al. A detailed analysis of the Gl 486 planetary system. *A&A* **2022**, *665*, A120. [[CrossRef](#)]
39. Castelli, F.; Kurucz, R.L. New Grids of ATLAS9 Model Atmospheres. In *Modelling of Stellar Atmospheres, Poster Contributions, Proceedings of the 210th Symposium of the International Astronomical Union, Uppsala University, Uppsala, Sweden, 17–21 June 2002*; Piskunov, N., Weiss, W.W., Gray, D.F., Eds.; Published on behalf of the IAU by the Astronomical Society of the Pacific; Cambridge University Press: Cambridge, UK, 2003; Volume 210, p. A20. <https://arxiv.org/abs/astro-ph/0405087>.
40. Baraffe, I.; Homeier, D.; Allard, F.; Chabrier, G. New evolutionary models for pre-main sequence and main sequence low-mass stars down to the hydrogen-burning limit. *Astron. Astrophys.* **2015**, *577*, 4–9. [[CrossRef](#)]
41. Cifuentes, C.; Caballero, J.A.; Cortés-Contreras, M.; Montes, D.; Abellán, F.J.; Dorda, R.; Holgado, G.; Zapatero Osorio, M.R.; Morales, J.C.; Amado, P.J.; et al. CARMENES input catalogue of M dwarfs. *Astron. Astrophys.* **2020**, *642*, A115. [[CrossRef](#)]
42. Bayo, A.; Rodrigo, C.; Barrado Y Navascués, D.; Solano, E.; Gutiérrez, R.; Morales-Calderón, M.; Allard, F. VOSA: Virtual observatory SED analyzer. An application to the Collinder 69 open cluster. *Astron. Astrophys.* **2008**, *492*, 277–287. [[CrossRef](#)]
43. Villanueva, G.L.; Smith, M.D.; Protopapa, S.; Faggi, S.; Mandell, A.M. Planetary Spectrum Generator: An accurate online radiative transfer suite for atmospheres, comets, small bodies and exoplanets. *J. Quant. Spectrosc. Radiat. Transf.* **2018**, *217*, 86–104. [[CrossRef](#)]
44. Kasting, J.F.; Brown, L.L., The early atmosphere as a source of biogenic compounds. In *The Molecular Origins of Life: Assembling Pieces of the Puzzle*; Brack, A., Ed.; Cambridge University Press: Cambridge, UK, 1998; pp. 35–56. [[CrossRef](#)]
45. Kasting, J.F. Runaway and moist greenhouse atmospheres and the evolution of Earth and Venus. *Icarus* **1988**, *74*, 472–494. [[CrossRef](#)]
46. Taniguchi, M.; Lindsey, J.S. Absorption and Fluorescence Spectral Database of Chlorophylls and Analogues. *Photochem. Photobiol.* **2021**, *97*, 136–165. [[CrossRef](#)] [[PubMed](#)]
47. Sirohiwal, A.; Berraud-Pache, R.; Neese, F.; Izsák, R.; Pantazis, D.A. Accurate Computation of the Absorption Spectrum of Chlorophyll a with Pair Natural Orbital Coupled Cluster Methods. *J. Phys. Chem. B* **2020**, *124*, 8761–8771. [[CrossRef](#)]
48. Mirkovic, T.; Ostroumov, E.E.; Anna, J.M.; van Grondelle, R.; Govindjee.; Scholes, G.D. Light Absorption and Energy Transfer in the Antenna Complexes of Photosynthetic Organisms. *Chem. Rev.* **2017**, *117*, 249–293. [[CrossRef](#)]
49. Kurashov, V.; Ho, M.Y.; Shen, G.; Piedl, K.; Laremore, T.N.; Bryant, D.A.; Golbeck, J.H. Energy transfer from chlorophyll f to the trapping center in naturally occurring and engineered Photosystem I complexes. *Photosynth. Res.* **2019**, *141*, 151–163. [[CrossRef](#)]
50. Claudi, R.; Alei, E.; Battistuzzi, M.; Cocola, L.; Erculiani, M.S.; Pozzer, A.C.; Salasnich, B.; Simionato, D.; Squicciarini, V.; Poletto, L.; et al. Super-Earths, M Dwarfs, and Photosynthetic Organisms: Habitability in the Lab. *Life* **2021**, *11*, 10. [[CrossRef](#)] [[PubMed](#)]
51. Kopparapu, R.K.; Ramirez, R.; Kasting, J.F.; Eymet, V.; Robinson, T.D.; Mahadevan, S.; Terrien, R.C.; Domagal-Goldman, S.; Meadows, V.; Deshpande, R. Habitable Zones around Main-sequence Stars: New Estimates. *Astrophys. J.* **2013**, *765*, 131. [[CrossRef](#)]
52. McKay, C.P. Requirements and limits for life in the context of exoplanets. *Proc. Natl. Acad. Sci. USA* **2014**, *111*, 12628–12633. Available online: <https://www.pnas.org/content/111/35/12628.full.pdf> (accessed on 22 November 2022). [[CrossRef](#)] [[PubMed](#)]
53. Hashimoto, G.L.; Abe, Y.; Sugita, S. The chemical composition of the early terrestrial atmosphere: Formation of a reducing atmosphere from CI-like material. *J. Geophys. Res. Planets* **2007**, *112*, 5010. [[CrossRef](#)]
54. Henry, T.J.; Jao, W.C.; Subasavage, J.P.; Beaulieu, T.D.; Ianna, P.A.; Costa, E.; Méndez, R.A. The Solar Neighborhood. XVII. Parallax Results from the CTIOPI 0.9 m Program: 20 New Members of the RECONS 10 Parsec Sample. *Astron. J.* **2006**, *132*, 2360–2371. [[CrossRef](#)]
55. Reylé, C.; Jardine, K.; Fouqué, P.; Caballero, J.A.; Smart, R.L.; Sozzetti, A. The 10 parsec sample in the Gaia era. *A&A* **2021**, *650*, A201. [[CrossRef](#)]